Nanoscale

Accepted Manuscript

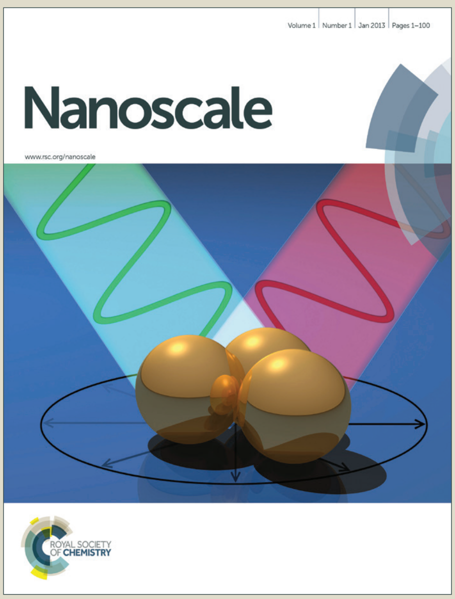

Journal Name RSCPublishing

ARTICLE

Spectral selectivity of 3D magnetophotonic crystal film fabricated from single butterfly wing scales

Cite this: DOI: 10.1039/x0xx00000x

Received 00th January 2012,
Accepted 00th January 2012

DOI: 10.1039/x0xx00000x

www.rsc.org/

Wenhong Peng,[a] Shenmin Zhu,[a] * Wang Zhang,[a] Qingqing Yang,[a] Di Zhang,[a] * Zhixin Chen[b]

3D magnetophotonic crystal (3D-MPC) film is an excellent platform for tailoring the magneto-optical response of magnetic materials. However, its fabrication is a great challenge due to the limitation of commonly used artificial synthesis methods. Inspired by the unique structures of biospecies, we hereby manipulate the pristine single wing scales of *Morpho didus* precisely and successful fabricate the Fe_3O_4 films with photonic structure. The synthesis strategy involves the fabrication of Fe_2O_3 film from a single wing scale using an improved sol-gel method followed by a subsequent reduction. The intrinsic hierarchical photonic structures as well as the anisotropic optical properties of the pristine butterfly wing scale have been retained in the obtained Fe_2O_3 and Fe_3O_4 films. When investigated under an external magnetic field, a spectral blue shift about 43 nm is observed in designated orientation of the Fe_3O_4 film, which is useful for the design and creation of novel magnetic-optical modulator device. Furthermore, these single scales can be used as building blocks to fabricate designable and more complicated assembled nano systems. This biomimetic technique combined with a variety structure of butterfly wings scales provides an effective approach to produce magneto-photonic films with desired structure, paving a new way for the theoretical research and practical applications.

Introduction

Magnetophotonic crystals (MPC) have attracted great interest for its potential applications in optoelectronics, in which the electromagnetic waves can be controlled by MPC structures.[1] By judicious material design, it is possible to control the light propagation and modify the magneto-optical spectral response. As a result, MPC is an ideal platform for the development of a new generation isolators for optical data transmission and integrated optics.[2] Among them, MPC with a three dimensional (3D) are of particular interest, because they give the possibility for the 3D control of the visible light in real time under a magnetic field. Unfortunately, 3D photonic crystals of ferromagnetic particles, such as Fe_3O_4, cannot be synthesized easily in principle because of strong magnetic attractive interactions between Fe_3O_4 particles. To balance the magnetic attractive force, approaches such as the ferrofluid in aqueous solution or non-polar solvents, have been developed in synthesizing MPC.[3, 4] Early in 2004, Inoue *et al.* introduced magnetic materials into an existing opal photonic crystal to obtain a opal-magnetite composite, which showed considerable changes in the Faraday rotation inside the photonic band gap.[5, 6] Though a significant progress has been achieved, most of the researches only focused on introducing magnetic defect to the multi-layer and opal structure and the synthesized monotonous structures greatly limit the investigation and possible application of MPC. Methods that can be used to make MPC with hierarchical photonic crystal to operate in the visible spectrum are highly desirable. However, manufacture of these materials remains a challenging and expensive task for currently available artificial laboratory techniques.

Actually, a variety of photonic crystals that can work in the visible wavelength range happen to be abundant in nature. Sea mouse, beetles, peacock feather and butterflies are some typical examples with periodic dielectric structures.[7-9] The blue wings of the *Morpho* butterfly species are one of the most well-known examples exhibiting brilliant structural color.[10, 11] These colors originate from 3D periodic sub-microstructures in every single wing scales (SWSs) rather than from pigments. Replicating such 3D periodic sub-microstructures in functional oxides and metals from *Morpho* butterfly wings is proved to be an efficient approach for fabricating functional materials with unique optical properties. The effectiveness of the replication approach has been manifested by the successful fabrication of 3D rutile titania,[12] 3D metallic butterfly wing scales with hierarchical sub-micrometer structures[13, 14] and Iridescent ZrO_2.[15] Very recently, we fabricated a magneto-photonic crystal from *Morpho* butterfly wings which consisted of 3D networks of magnetite nanoparticles.[16] Importantly, it has been shown that the photonic band gap of the 3D magnetite networks could be tuned by an external magnetic field. However, all these spectrometer results in the cited works were based on a whole butterfly wings rather than SWSs. As we know, a whole butterfly wings are usually composed of more than one layers, like roof-tiles, including top and bottom layers (dorsal and ventral surfaces) that both contain two or even more different kinds of overlapping scales, and a middle layer (wing membrane) for fixing and supporting the scale. Different scales in a whole butterfly wing have various periodic microstructures. The narrow width of the ridges, random variations in the exact shape of each ridge and pigment in the scales, cause the butterfly wings to exhibit not only interference, but also diffraction, scattering, and even pigment-induced absorption, which all work together to produce the paradox of colorful, yet angle-independent iridescence of butterflies. SWSs are the functional cells in a butterfly wing system to control and manipulate visible light. For instance, the cover scale of *Morpho didius* can be used to diffuse light merely in one plane and make the range of reflection narrower in the orthogonal plane.[17] The synthesized replicas in these cited works were stacked biological parts and hard to separate because of the fragility of the inorganic materials. What's more, the properties of these reported butterfly replicas were difficult to scientifically characterize, especially the optical properties after replica formation. Recently, a *sol-gel* technique was developed for the fabrication of ZnO and ZrO_2 replicas using a SWS as the template.[18, 19] The single wing replica showed spatial optical anisotropy property which has never been found in the replica from a whole butterfly wing.[15, 20] All these reasons stimulate a deeper and specific study to directly fabricate and evaluate the magnetic and optical properties of individual SWS magnetite replicas.

Unfortunately, the previous approaches are not suitable for the fabrication of Fe_3O_4 film with photonic crystal for at least two reasons below. First, the precisely manipulating a SWS is a great challenge, especially after combining with the sol-gel precursor solution, the SWSs hybrid can be easily stacked together firmly. Second, the magnetic interaction force between the Fe_3O_4 nanoparticles, that is, the attractive force restricts the formation of photonic structures. Here, we address the above challenge by carefully picking a SWS precursor out from a hybrid whole butterfly wing in combination of a reduction process. For the first time, we report a new class of magnetic photonic crystal nanosystem by templating from SWSs. The factors that influence the precise replication of SWS Fe_3O_4 film are investigated and discussed. The hierarchical photonic structure of the pristine wing scale is faithfully replicated by the intermediate Fe_2O_3 film and final MPC-Fe_3O_4 film. The optical responses of these MPC-Fe_3O_4 film and intermediate Fe_2O_3 film are measured and they demonstrate a highly spatial optical anisotropy. The effect of an external magnetic field on the photonic band gap of the MPC-Fe_3O_4 film in the visible light range is also investigated. It is shown that the reported SWS template technique provides an effective approach for the synthesis of the functional materials with desired photonic crystals structures.

Experiment

Chemicals and reagents

The butterfly wing scales chosen as bio-templates are from *Morpho Didius*, which were purchased from a butterfly garden in Shanghai. Water was deionized by a Nano Pure System. Ferric chloride, acetic acid and ethanol were from the Guo Yao Chemical Reagent Company. Silicon substrates and Needle were purchased from a Taobao shop. All reagents used in this experiment were of analytical grade without further purification.

Preparation of iron oxides single wing scale

The whole fabrication process contains five main steps (Scheme 1): pretreatment of the pristine butterfly wings, self-assembling of Fe_2O_3 seed particles; selection of single scales; heat treatment in air to remove bio-template and final reduction process to get Fe_3O_4 cover scale. In the first step, butterfly wings needed to be pre-treated by 60% acetic acid ethanol solution for 4 h in ambient condition in order to remove additional impurities covered on the wings. In the second step, Fe_2O_3 alcosol was produced by dissolving $FeCl_3{\cdot}6H_2O$ in water-free ethanol with the molar ratio of ethanol to $FeCl_3{\cdot}6H_2O$ 1:0.3 at 60 °C for 15 minutes under magnetic stirring. The pre-treated butterfly wings were dipped into the Fe_2O_3 alcosol for 24 h. Then the socked butterfly wings were taken out and washed with deionized water. In the third step, the butterfly wings were dried under vaccum overnight at room temperature, and a single scale from the dried wings was picked up using an acupuncture needle under an optical microscope. A drop of ethanol with diameter of 50 μm was pre-dropped onto the silicon substrate. The single scale on the needle tip was then transferred onto the surface of the pre-prepared drops and finally adhered tightly onto the substrate as the liquid evaporated. Next, the as prepared single scale sample was calcined at 500°C for 3 h in air, leaving hematite in the form of ceramic wing scale. Finally, a magnetite SWS was obtained by a heat treatment of the hematite single scale under a H_2/Ar (1:4 volume ratio) flow at 400 °C for 1 h. In order to characterize the phase of the final product, Fe_3O_4 replica from a whole butterfly wing was also synthesized at the same condition as above to collect the powder for the X-ray diffraction.

Characterization

The as-synthesized samples were then examined by SEM, and FESEM images were obtained on an FEI Quanta FEG 250 SEM at 20 kV. Chemical composition was measured using energy dispersive X-ray spectroscopy (EDS) on an FEI Quanta FEG 250 SEM at 20 kV. Optical images were obtained on a digital optical microscope (Keyence VHX-1000). For cross-sectional structure analysis, after embedding the wings in epoxy, a Cryo-ultramicrotome (Leica ULTRACUT UC6) was used to slice the cross-sectional samples for analysis using Bio-TEM (FEI Tecnai G2 spirit Biotwin). Angle resolved reflectance spectra were acquired using a CRAIC QDI 2010 UV-visible-near infrared microspectro photometer. Magnetization curves were recorded using a Physical Property Measurement System (PPMS-9T, Quantum Design Inc., USA).

Results and Discussion

Selection of single wing scales

Morpho butterfly wings have been widely studied owing to their iridescent attractive structure color.[21, 22] Under the microscope, it is shown in Fig. 1a that the wings are covered by two kinds of scales. The highly reflective arrays of blue scales on the ground layer are called ground scales, whereas the transparent scales with bluish lie above the ground scales forming a second layer are known as cover scales (Fig. 1b). The main structure on the both scales is the ridges connected by cross ribs. As depicted in Fig. 1g, the cross section of the ridge resembles the "Christmas tree". The major structural difference between the cover and ground scales lies in the density of the cross ribs in between two nearby ridges. The density of the cross ribs in the ground scale is almost twice those in the cover scale.[23] In addition, the lamellae have a uniform width from the top to the root in the cover scales, while the lamellae width in the ground scales increases gradually from the top to the root (Fig. S1). The ground scales are also much thicker. Importantly the base plate of the cover scale is flat but that of the ground scale is irregularly curvy. Finally, they have different optical functionalities; the ground scales are responsible for broadening observable directions and providing the main blue color of butterfly wing[24, 25] and the cover scales gives the blue color to the wing through their wavelength-selective mechanism and anisotropic light-diffusing character.[17] Functioning as an anisotropic optical diffuser, the cover scale can diffuse light merely on one plane and narrow reflection range on the orthogonal plane. This is why the cover scale is chosen for this investigation.

Structure of the cover scale of *Morpho didius*

Fig. 1c shows an optical image of a single cover scale. It has a typical dimension of ~150 μm in length and ~60μm in width. Thirty to thirty five rows of lamellae align on the each scale surface with almost an identical interspacing. A closer view of these lamellae in the cover scale is illustrated in Fig. 1e-f. To facilitate the description, a reference coordinate system is introduced and defined as in Fig. 1d. Fig. 1e is a SEM image from the top view of a cover scale on x-y plane, showing that the spacing between lamellae is ~1.7μm and they are supported by a numbers of cross ribs. In addition, Fig. 1f shows a SEM image from the side view of the cover scale on x-z plane. The cuticle layers have a width of about 300 nm and thickness of 100-120 nm with an air gap of 60-90 nm. These layers are found to run obliquely to the base plate with the tilt angle 7°, based on the estimation from the length of the layer and height of the ridge. The cross-section of the cover scale is shown in Fig. 1g revealing that the ridges are joined at their intersection by the cross ribs. Eighteen lamellae decorating both sides of the ridges are also visible. With an average thickness of 90 nm, they appear alternately on both sides of ridges. The distance between two adjacent lamellae (at the same side of ridges) is approximately 90 nm.

Fabrication and morphologies of Fe_2O_3 & Fe_3O_4 replicas

In this work, Fe_2O_3 and Fe_3O_4 replicas were synthesized from individual single cover scales and their angle-dependent reflective properties were investigated. For the purpose of comparison, Fe_2O_3 and Fe_3O_4 replicas are also fabricated from ground scales and a whole butterfly wing using the same process.

It is quite interesting that the fabrication of Fe_2O_3 from single wing scales is considerably different from a whole wing. The key to the successful fabrication of Fe_2O_3 from SWSs is to place the wing scales evenly onto a smooth surface to ensure that the surface of the single wing scales does not curl during the heat treatment.

It is known that the periodic size of photonic crystal structures determines their optical properties. During the synthesis process, a shrinkage of periodic size is inevitable in the annealing process (to remove the pristine bio-templates) because of the decomposition of chitin (main components in butterfly's wings) at high temperatures[12] and it leads to the distortion of the photonic crystal structure of the resulting replica scales. The distortion prevents the replicated butterfly from inheriting the ingenious optical properties of the natural wing scales. Furthermore, the complicated combination modes like the overlap photonic crystal structures make the optical properties of the ceramic butterfly wings powder and film very difficult to scientifically characterize if it is possible. To the best of our knowledge, ceramic butterfly wings made from a whole butterfly wing show no anisotropic optical properties,[16, 26-28] although the anisotropic optical properties of the biological butterfly wings were demonstrated experimentally[29] and theoretically.[24] Thus, it is imperative to develop a method that can control the contraction during the removal of the pristine templates. Therefore it is necessary to attach SWSs onto a flat substrate surface evenly and tightly before the removal of the natural template in order to keep the periodicity of the scales unchanged in one direction (determined by main ridges) and minimizes the contractions within certain directions.

The morphology of the Fe_2O_3 scale was investigated on a SEM and the results are illustrated in Fig. 2a-d. The ground scale replica was listed in the support information for the sake of comparison. As compared with the pristine cover scale (Fig. 1c), the Fe_2O_3 replica retained the overall single-scale shape, parallel ridges and nano-scale ribs of the bio-template (Fig. 2a). The zoom-in SEM images (Fig. 2b-c) reveal that the inter-lamellae spacing remained approximately 1.7 μm for the Fe_2O_3 replica. Change in the spacing is hardly observed, when compared with their pristine natural chitin-based counterpart in Fig. 1d. Fig. 2d is a side-view image of the as-synthesized Fe_2O_3 replica at a considerable high magnification, where the sub-microstructure of the main ridges can be observed. The width of the main ridges themselves shows 30% shrinkage during the fabrication process, changing from 300 nm (pristine scale) to 200 nm (Fe_2O_3 replica). The size of the sub-ribs is marked in Fig. 2. The results indicate a near precise replication of the pristine butterfly wing's subtle structure in the Fe_2O_3 replica. During the synthesis process, it is found that the Fe_2O_3 cover scale could be laid evenly on a flat Si-substrate and the basement membrane is adhered tightly to the Si-substrate. A Fe_2O_3 replica is also made from a ground scale template in the same way as that from the cover scale. Optical and SEM images of the Fe_2O_3 replica are given in Fig. S2. It is found that the Fe_2O_3 replica templated from the ground scale cracked, curled up and eventually peeled off from the Si substrate. This is because the substrate membrane of the ground scale is not flat enough so that it cannot contact with the Si substrate tightly as shown in Fig. S3. As can be seen, there are cavities between the substrate membrane and the Si substrate. Consequently, the ground scale can easily upturn and the Fe_2O_3 replica peels off from the Si substrate during the fabrication process.

A Fe_3O_4 replica film is obtained by treating the Fe_2O_3 replica at 400 °C in a mixed H_2 /Ar gas. Consequently, the ferric ion is partially reduced by H_2. FESEM (Field Emission Scanning Electron Microscopy) images in Fig. 3 indicate that the Fe_3O_4 replica exhibits a well-organized framework with parallel ridges and pillars, which are faithfully replicated from the natural cover scale (Fig. 3a-b). The structural details of the single scale replica are illustrated in Fig. 3b-c. The inter-lamellae spacing is measured to be about 1.7 μm (Fig. 3c), and almost the same as that of the Fe_2O_3 replica (Fig. 2c) and the natural untreated cover scale (Fig. 1c). No shrinkage is detected in the Fe_3O_4 replica (Fig. 3a-b). Thus, the photonic structures of SWSs are replicated with a very high fidelity. To the best of our knowledge, this is the first time that a SWS Fe_3O_4 replica is synthesized.

Compared to the replica from a whole butterfly wing, the subtle structure which plays a vital role in the angular reflectance can be retained more faithfully in the replica from cover scale. Furthermore, the replica from a whole butterfly wing is too fragile for potential applications.

Reflectance characterization

In order to investigate the dependence of the reflectivity under incidence light, goniometric measurements were carried out. The goniometric reflectance measurements are performed under the arbitrarily-chosen 85° angle of the incidence with respect to the wing plane using a QDI 2010 UV-visible-near infrared micro-spectrophotometer (xenon light source, non-polarized) as shown in Fig. 4a. Similar setups can be found in ref.[30, 31] The wing scale has 2-fold rotation symmetry around z-axis. In order to take a full reflectance spectrum therefore it is sufficient to rotate the scale about the z-axis every increment of 10° until the total rotation of 180° is reached.

Fig. 4f and g depict the reflectance spectra of the natural cover scale. There are remarkable differences in the spectra, in terms of angular positions and amplitudes of the reflectance maxima. When θ changes from 30° to 150°, the reflection spectrum reaches a maximum intensity around 457 nm at θ =110°. From 60 to 110°, the reflectance peak blue-shifted from 492 to 457 nm with the continuously increase of the reflectance intensity (Fig. 4f). From 110° to 140°, the reflection peak has a slight red shift from 457 to 472 nm with the continuous decrease of the reflectance intensity (Fig. 4g). These effects may be associated to a certain extent with the changes in the projected periodicity as the scale is rotated. For the cover scale, it has a highly anisotropic microstructure and the rotation plane deviates from the plane of the scale membrane by an angle around 7°.[26]

The reflection measurements are also performed on the Fe_2O_3 and Fe_3O_4 replicas in the visible and near-IR regions to study the interaction of the synthesized replicas with light. We keep the φ fixed at 85° and change the incidence (rotation) angle θ. Both the magnetite replica and Fe_2O_3 replica preserve the anisotropic optical properties of their natural counterparts well. Fig. 5a-e shows the optical images of the Fe_2O_3 replica under different incident angles. The color of the Fe_2O_3 replica consists of a number of small color pixels, which originates from the sub-micron structures of individual scales. The Fe_2O_3 replica exhibits its highest reflection at 630-700 nm and secondary peak at 420-470 nm (Fig. 5f and g), showing the consistency with color pixels observed in the optical images (Fig. 5a and e). The main peak of the Fe_2O_3 replica red-shifts with a narrower width, as compared with that of the natural wing scales (Fig. 4). The appearance of these two peaks suggests that the synthesized Fe_2O_3 replica possesses at least two kinds of periodicity. This is consistent with the fact that the pristine and organic lamellar lattice (chitin, RI = 1.56) are replaced by air and the Fe_2O_3 matrix, which has a higher RI (3.05). Our results show the reflectance maxima of the Fe_2O_3 scales slight blue-shift from 665 to 646 nm when the rotation angle θ changes from 145° to 190°. Such an angular dependence on the reflectance is the characteristics of structural color, indicating that the Fe_2O_3 replica kept the structural fidelity of the natural butterfly wing.

The reflectance spectra of the final Fe_3O_4 replica are measured with θ ranging from 60° to 190°. Beyond this angular range, the replica displays negligible reflections. The Fe_3O_4 replica displays reflection peaks center at 680-720 nm (Fig.5h and i). They have lower intensities than the natural cover scale and the intermediate Fe_2O_3 replica, because of the black physical color or the low refractive index 2.4 of Fe_3O_4 nanoparticle. The result is consistent with our previous study on the intact Fe_3O_4 butterfly wing.[16] Previous studies[26] have indicated that the location of the band-gap is determined by the width of the periodic ridges of the scale (the ‘‘trunk’’ of the tree-like structure), the thickness of the lamellae (the ‘‘branches’’ of the tree-like structure), and the refractive index of the material. Increasing the refractive index without changing the lattice size should lead to the band-gap red-shift, the increase in the reflectance intensity, and broadening the band-gap. In contrast, simply reducing or increasing the lattice size should lead to a blue or red band-gap shift, respectively. Since the photonic structure of the cover scale is an irregular one, the present results are quite reasonable. This is the first time that Fe_3O_4 cover scale is successfully fabricated and shows anisotropic optical properties.

Fig. 5j and k show typical reflection spectra of the Fe_3O_4 photonic crystals in response to a varying magnetic field through changing the distance between an NdFeB magnet and the sample from 2 to 4 cm. Two optical responses are observed. The reflectance peak under an external magnetic field has a sharp blue-shift from 699 to 656 nm when the rotational angle shifts from 140° to 130°. On the other hand, the reflectance intensity of the Fe_3O_4 replica is slightly reduced. The sharp blue-shifted peak is induced by the external magnetic field, may be explained by the interaction between the magnetic Fe_3O_4 and the external field causing the distortion of the photonic crystal structure. The detailed mechanisms need further study in the future.

A Physical Property Measurement System is used to study the magnetic properties of the Fe_3O_4 cover scale. From the magnetization curve shown in Fig. 6, it is found that the single wing replica on the Si substrate shows apparent magnetic properties. The Fe_3O_4 replica powder from a whole butterfly wing is characterized by XRD (Fig. S4), and the results confirm the components of the final replica consist of almost pure magnetite.

Conclusion

In summary, we have developed a novel approach to synthesize 3D photonic magnetite film from a single butterfly wing cover scale. The obtained magnetite Fe_3O_4 film and intermediate hematite Fe_2O_3 film preserve the morphology and anisotropic optical properties of the cover scale fidelity. Interestingly, a spectral blue shift about 43 nm is observed in the Fe_3O_4 film when the rotational angle shifts from 140° to 130° under an external magnetic field, implying an optical and magnetic coupling effect and magnetically tunable photonic properties of the ceramic cover scale. The combination of natural photonic structures with functional materials can provide an effective approach to produce magnetophotonic films, which paves a new way for theoretical research and practical applications in specific optical, magnetic, and electric devices.

Figures and Scheme

Scheme 1. Schematic illustration of the replication process of single *Morpho* butterfly wing scale

Fig. 1 Morphology and structure of the pristine butterfly wing (*Morpho didius*) and its cover wing scales. (a) Optical image of the scales at the blue area of the *M. didius* wing, revealing two types of wing scales (cover scale and ground scale). (b) SEM image of cover and ground scales. (c) Optical image of a cover scale. (d) Orientation of a butterfly wing in a reference coordinate system. The sample is placed on the x-y plane with the z-axis being normal, and the x-axis is defined along the lamellae running length of the scale from root to tip. The light propagation direction, represented by the red arrow, is determined by two angles: the polar angle θ on the x-y plane and the azimuth angle 90°-φ on x-z plane. (e) SEM image from the top view of cover scale on x-y plane. (f) SEM image from the side view of cover scale on x-z plane. (g) TEM image of cross section of cover scale on y-z plane.

Fig. 2 Microstructure of Fe_2O_3 cover scale, (a)-(c) SEM images (for comparison, refer to the pristine butterfly wing scale in Fig. 1b-c), (d) SEM image of the side view of a Fe_2O_3 replica. It should be noted that space (1.7μm) between main ridges is virtually the same as that of the pristine wing scale (see Fig. 1c). SEM images of intact Fe_2O_3 replica were listed in the support information.

Fig. 3 Microstructure of Fe_3O_4 cover scale, (a)-(c) SEM images, which can be compared with a natural butterfly wing scale in Fig. 1b-c, (d) SEM image of the side view of a Fe_3O_4 replica. It should be noted that spaces (1.7μm) between main ridges are well kept as compared with their pristine and Fe_2O_3 replica counterparts (see Fig. 1c, Fig. 2d).

Fig. 4 (a) shows the schematic geometry for the goniometric reflectance measurements. The orientation of the scales is shown schematically by the red ladders. The illumination angle was arbitrarily chosen to be 85° on the x-z plane. The wing cover scale was rotated around the z-axis, a reflectance spectrum was taken in every 10° rotation until 150°; (b)-(e) show the optical images of single wing cover scale taken at θ = 30, 70, 90 and 100° respectively; (f) and (g) show the reflectance spectra taken at angles θ between 30-150°.

Fig. 5 Optical characterization of the Fe_2O_3 replicas of cover scales. (a)-(e) Optical images of a Fe_2O_3 scale replica illuminated with different incident angles. Angle dependent reflectance spectra of the single wing Fe_2O_3 replica (f) and (g), single wing Fe_3O_4 replica without external magnetic field (h) and (i) Fe_3O_4 replica under external magnetic field (j) and (k) .The incidence angle was fixed at φ=85°, and the reflectance was measured from (f) 110° to 145° and (g)145° to 190°, respectively.

Fig. 6 Magnetization curve of the obtained Fe_3O_4 SWSs replica.

Acknowledgements

The authors gratefully acknowledge the financial support Morgan Crucible Company, the National Science Foundation of China (Nos. 51171110, 51072117), the National Basic Research Program of China (973 Program, 2012CB619600),Research Fund for the doctoral program of higher education of China(20120073130001), Shanghai Science and Technology Committee(No. 10JC1407600, 13JC1403300). The authors also thank SJTU Instrument Analysis Center for Cryo-ultramicrotome and Bio-TEM measurements.

Notes and references

[a] State Key Lab of Metal Matrix Composite, Shanghai Jiao Tong University Shanghai, 200240, (China) E-mail: smzhu@sjtu.edu.cn; zhangdi@sjtu.edu.cn

[b] Faculty of Engineering and Information science, University of Wollongong, Wollongong, NSW, 2522, (Australia)

†

Electronic Supplementary Information (ESI) available: SEM, Optical image of ground scale, XRD of the magnetite with butterfly wing structure. See DOI: 10.1039/b000000x/

1. M. Inoue and T. Fujii, *J. Appl. Phys.*, 1997, **81**, 5659-5661.
2. M. Inoue, H. Uchida, K. Nishimura and P. B. Lim, *J. Mater. Chem.*, 2006, **16**, 678-684.
3. J. Ge, L. He, J. Goebl and Y. Yin, *J. Am. Chem. Soc.*, 2009, **131**, 3484-3486.
4. J. Ge, Y. Hu, T. Zhang, T. Huynh and Y. Yin, *Langmuir*, 2008, **24**, 3671-3680.
5. T. Kodama, K. Nishimura, A. V. Baryshev, H. Uchida and M. Inoue, *Phys. Status Solidi B)*, 2004, **241**, 1597-1600.
6. A. Baryshev, T. Kodama, K. Nishimura, H. Uchida and M. Inoue, *Magnetics, IEEE Transactions on*, 2004, **40**, 2829-2831.
7. R. McPhedran, N. Nicorovici, D. McKenzie, L. Botten, A. Parker and G. Rouse, *Aust. J. Chem.*, 2001, **54**, 241-244.
8. J. Zi, X. Yu, Y. Li, X. Hu, C. Xu, X. Wang, X. Liu and R. Fu, *PNAS*, 2003, **100**, 12576-12578.
9. L. P. Biro and J.-P. Vigneron, *Laser Photonics Rev.*, 2011, **5**, 27-51.
10. A. Parker, JOptA, 2000, **2**, R15-R28.
11. A. D. Pris, Y. Utturkar, C. Surman, W. G. Morris, A. Vert, S. Zalyubovskiy, T. Deng, H. T. Ghiradella and R. A. Potyrailo, *Nat Photon*, 2012, **6**, 195-200.
12. M. R. Weatherspoon, Y. Cai, M. Crne, M. Srinivasarao and K. H. Sandhage, Angew. *Chem. Int. Ed.*, 2008, **47**, 7921-7923.
13. Y. Tan, J. Gu, X. Zang, W. Xu, K. Shi, L. Xu and D. Zhang, *Angew. Chem.*, 2011, **123**, 8457-8461.
14. Z. Mu, X. Zhao, Z. Xie, Y. Zhao, Q. Zhong, L. Bo and Z. Gu, *J. Mater. Chem.B*, 2013.
15. Y. Chen, *Appl. Phys. Lett.*, 2009, **94**, 053901.
16. W. Peng, S. Zhu, W. Wang, W. Zhang, J. Gu, X. Hu, D. Zhang and Z. Chen, *Adv. Funct. Mater.*, 2012, n/a-n/a.
17. S. Yoshioka and S. Kinoshita, *Proc. R. Soc. Lond. B Biol. Sci.*, 2004, **271**, 581-587.
18. Y. Chen, X. Zang, J. Gu, S. Zhu, H. Su, D. Zhang, X. Hu, Q. Liu, W. Zhang and D. Liu, *J. Mater. Chem.*, 2011, **21**, 6140-6143.
19. Y. Chen, J. Gu, D. Zhang, S. Zhu, H. Su, X. Hu, C. Feng, W. Zhang, Q. Liu and A. R. Parker, *J. Mater. Chem.*, 2011, **21**, 15237-15243.
20. W. Zhang, D. Zhang, T. Fan, J. Ding, J. Gu, Q. Guo and H. Ogawa, *Bioinspir. Biomim.*, 2006, **1**, 89.
21. S. Kinoshita, S. Yoshioka and J. Miyazaki, *Rep. Prog. Phys.*, 2008, 71, 076401.
22. S. Kinoshita, S. Yoshioka, Y. Fujii and N. Okamoto, *FORMA-TOKYO-*, 2002, **17**, 103-121.
23. S. Berthier, E. Charron and A. Da Silva, *Opt. Commun.*, 2003, **228**, 349-356.
24. W. Wang, W. Zhang, W. Chen, J. Gu, Q. Liu, T. Deng and D. Zhang, *Opt. Lett.*, 2013, **38**, 169-171.
25. P. Vukusic, J. Sambles, C. Lawrence and R. Wootton, *Proc. R. Soc. Lond. B Biol. Sci.*, 1999, **266**, 1403-1411.

26. J. Huang, X. Wang, and Z. L. Wang, *Nano Lett.*, 2006, **6**, 2325-2331.
27. C. Mille, E. C. Tyrode and R. W. Corkery, *RSC Advances*, 2013, **3**, 3109-3117.
28. G. Cook, P. L. Timms and C. Göltner - Spickermann, *Angew. Chem. Int. Ed.*, 2003, **42**, 557-559.
29. S. Kinoshita, S. Yoshioka and K. Kawagoe, *Proc. R. Soc. Lond. B Biol. Sci.*, 2002, **269**, 1417-1421.
30. C. Lawrence, P. Vukusic and R. Sambles, *Appl. Opt.*, 2002, **41**, 437-441.
31. K. Kertész, Z. Bálint, Z. Vértesy, G. I. Márk, V. Lousse, J. P. Vigneron, M. Rassart and L. P. Biró, *Phys. Rev. E*, 2006, **74**, 021922.

